PLANT SCIENCE TODAY
Vol 13(1): 1-6
https://doi.org/10.14719/pst.12262

eISSN 2348-1900

RESEARCH ARTICLE

Green synthesis and characterization of Fe_2O_3 and MgO nanoparticles

R Rajeshkumar[1], Pon Sathya Moorthy[2*], M Raveendran[3], G Karthikeyan[4], V Gomathi[1], M Djanaguiraman[5] & K Abinaya[1]

[1]Centre for Agricultural Nanotechnology, Tamil Nadu Agricultural University, Coimbatore 641 003, Tamil Nadu, India
[2]Department of Basic Engineering and Applied Sciences, Agricultural Engineering College & Research Institute, Kumulur 621 712,Tamil Nadu, India
[3]Department of Plant Biotechnology, Tamil Nadu Agricultural University, Coimbatore 641 003, Tamil Nadu, India
[4]Department of Plant Pathology, Tamil Nadu Agricultural University, Coimbatore 641 003, Tamil Nadu, India
[5]Department of Crop Physiology, Tamil Nadu Agricultural University, Coimbatore 641 003, Tamil Nadu, India

*Correspondence email - sathyamoorthy.pon@tnau.ac.in

Received: 14 October 2025; Accepted: 26 November 2025; Available online: Version 1.0: 27 January 2026; Version 2.0: 05 February 2026

Cite this article: Rajeshkumar R, Pon SM, Raveendran M, Karthikeyan G, Gomathi V, Djanaguiraman M, Abinaya K. Green synthesis and characterization of Fe_2O_3 and MgO nanoparticles. Plant Science Today. 2026; 13(1): 1-6. https://doi.org/10.14719/pst.12262

Abstract

Despite growing interest in metal oxide nanomaterials, there remains a notable lack of systematically engineered iron oxide (Fe_2O_3) and magnesium oxide (MgO) nanoparticles with well-defined structural and surface properties tailored for safe, multifunctional use in agriculture and environmental remediation. This study comprehensively evaluates the synthesis and characterization of Fe_2O_3 and MgO nanoparticles, revealing their successful formation with controlled crystallinity, morphology and surface functional groups. X-ray diffraction (XRD) analysis confirmed the nanocrystalline structures and high purity of both nanoparticles. Magnesium oxide showed sharp, well-defined peaks indexed to the cubic phase (JCPDS card no. 45-0946 with crystallite sizes 18-25 nm) using the Scherrer equation. The Fe_2O_3nanoparticles displayed sharp phase-specific peaks with crystallite sizes ranging from 20 to 35 nm, demonstrating their high purity and crystallinity. Fourier-transform infrared (FTIR) spectroscopy identified characteristic functional groups, including surface hydroxyls and metal-oxygen stretching vibrations. Mg-O (~411 cm^{-1}) and Fe-O bands confirmed reactive nanostructures. Transmission electron microscopy (TEM) images revealed predominantly hexagonal MgO nanoparticles sized 20-40 nm with sharp boundaries indicating low defects, while Fe_2O_3 nanoparticles exhibited near-spherical to polyhedral morphologies ranging from 23 to 64 nm, with moderate agglomeration attributed to magnetic interactions. These well-controlled nanostructures, with high surface area and reactivity, are promising candidates for agricultural and environmental applications, nanofertilizers, plant virus management, catalysis and remediation.

Keywords: Fe_2O_3 nanoparticles; Fourier-transform infrared spectroscopy (FTIR); MgO nanoparticles; nanocrystalline structure; nanoparticle morphology

Introduction

The eco-friendly synthesis of metal oxide nanoparticles using plant extracts has gained prominence as a sustainable and green alternative to conventional chemical methods due to its simplicity, cost-effectiveness and environmental compatibility (1, 2). In such biosynthetic approaches, plant-derived biomolecules including flavonoids, phenolics, terpenoids and alkaloids serve as reducing and stabilizing agents, avoiding the use of toxic reagents and harsh conditions (3). Among various medicinal plants, *Moringa oleifera* L. stands out as an excellent bio reductant due to its abundance of antioxidants, phenolic acids and secondary metabolites that facilitate efficient reduction of metal ions and stabilization of nanoparticles (4). The use of *M. oleifera* extract thus represents an eco-conscious and efficient route to synthesize stable, functional nanomaterials. Iron oxide nanoparticles (Fe_2O_3) produced through such green routes possess unique magnetic, catalytic and antimicrobial properties, making them suitable for applications in biomedicine, agriculture and environmental remediation (5). However, achieving stable, monodisperse Fe_2O_3 nanoparticles through entirely green synthesis remains a challenge. Similarly, magnesium oxide (MgO) nanoparticles are valued for their high surface reactivity and antimicrobial activity, yet conventional synthesis methods often involve energy-intensive and non-sustainable processes. The green synthesis of MgO nanoparticles using plant extracts provides a safer and more sustainable alternative, yielding materials with enhanced biocompatibility and reduced toxicity. Despite numerous studies, limited comparative research exists on Fe_2O_3 and MgO nanoparticles synthesized using the same biological source, which could provide insights into plant-mediated nanoparticle formation mechanisms. Therefore, the present study aims to synthesize Fe_2O_3 and MgO nanoparticles using *M. oleifera* leaf extract through an eco-friendly approach and to characterize their physicochemical properties using X-ray diffraction (XRD), Fourier transformed infrared spectroscopy (FTIR), scanning electron microscope (SEM), high resolution-transmission electron microscopy (HR-TEM), energy dispersive analysis of X-rays, Brunauer -Emmett-Teller and Raman spectroscopy. The biosafety of the

synthesized nanoparticles was also evaluated using beneficial microorganisms to ensure their suitability for sustainable applications.

Materials and Methods

Preparation of plant extracts (*M. oleifera*)

Preparation of plants extract was carried out for the synthesis Fe_2O_3 nano materials. After collecting fresh leaves of *M. oleifera*, respectively, they were washed thoroughly under running tap water to remove adhering dust and debris. The leaves were shade dried to remove the excess washed water. Shade dried leaves were incised into 1 cm × 1 cm, dimension. 100 g of leaves of *M. oleifera* were taken in 100 mL of glass beaker, respectively and boiled for 15 min at 100 °C. Whatman filter paper (No. 40) was used to filter and recover the extract individually and kept at 4 °C until used for Fe_2O_3 nanoparticle synthesis.

Synthesis of iron oxide nanoparticles

Ferric chloride (0.162 g) was dissolved in 100 mL of distilled H_2O to prepare 0.01 M $FeCl_3$solution. Above solution was mixed with equal volume of *M. oleifera* extract and stirred using a magnetic stirrer to ensure uniform mixing. The pH of the mixture was carefully maintained around 6 to facilitate optimal reduction and stabilization of iron ions. The solution was left undisturbed for 24 hr at room temperature to enable nanoparticle formation. Resulting solution was centrifuged at 7500 rpm for 15 min and the precipitate was recovered and washed 2-3 times with ethanol to remove the unreacted plant residues and impurities. The cleaned sample was then dried at 80 °C to remove moisture. Finally, the dried sample was calcined at 500 °C in a muffle furnace to obtain Fe_2O_3 nanoparticles (6).

Synthesis of MgO nanoparticles

Magnesium nitrate hexahydrate (1.8 g) was dissolved in 100 mL of distilled water to make up 0.2 M of magnesium nitrate solution. Sodium hydroxide (NaOH) solution (0.5 M) was prepared by dissolving 1 g of NaOH in 50 mL of distilled water. Sodium hydroxide (NaOH) solution was taken in a 50 mL burette and titrated against 0.2 M magnesium nitrate solution until pH reached to 14. The stirring process was continued for 30 min at 450 rpm at room temperature. The solution was centrifuged for 30 min at 7500 rpm to recover the precipitate. Recovered MgO was washed 3 times with ethanol and the sample was kept in muffle furnace for calcination at 350 °C for 4 hr (7).

Characterization of synthesized nanoparticles

The synthesized iron oxide nanoparticles were characterized by using (i) XRD for crystallographic analysis (ii) FTIR for functional group characterization (iii) TEM for size and internal structures.

(i) X-ray diffraction for crystallographic analysis

Powder X-ray diffraction (PXRD) was employed to determine the crystalline structure of the synthesized nanoparticles. Samples were irradiated with Cu-Kα radiation (λ = 1.54 Å) using a Shimadzu XRD-600 diffractometer. Approximately 500 mg of powder samples were put on a sample holder and characterized for this analysis. It employed 40 KV current, Cu-Kα radiation (λ = 1.54 Å), a sample width of 0.02 degrees, a scan speed of 1 degree per min and a scan range of 10 to 90 degrees. Bragg's law (nλ = 2d Sin θ) must be satisfied to produce constructive interference produced by the diffracted X-rays. Diffracted X-rays are allowed to fall on the detector to record the diffraction pattern of the sample. Data were processed using OriginPro 8.5 software.

(ii) Fourier Transformed Infrared Spectroscopy for functional group characterization

An FTIR spectrometer JASCO FTIR/6800- ATR Spectrometer (JASCO Japan) within the 400-4000 cm^{-1} spectral region, the averaged 64 scans spectra with a resolution of 4 cm^{-1}were used to analyse the sample.

(iii) Transmission Electron Microscopy for size and internal structures

Transmission electron microscope (Technai G2 T20 S-Twin - FEI, Netherlands) was used to analyse the structural features of the synthesized nanoparticles were investigated by positioning the sample on a copper grid. After that, images were obtained in bright-field mode at an accelerating voltage of 200 kV.

Results and Discussion

Characterization of Fe_2O_3 and MgO nanoparticle

Crystallographic analysis of Fe_2O_3 by XRD

Powder X-ray diffraction pattern of the synthesized Fe_2O_3 nanoparticles displayed sharp and well-defined peaks, confirming their crystalline nature. Prominent diffraction peaks were observed at 2θ values around 24.1°, 33.2° and 49.5°, corresponding to the (012), (104) and (024) planes of rhombohedral α-Fe_2O_3 (hematite), in alignment with JCPDS Card No: 33-0664. The most intense peak at around 33.2°, with a high count rate of 1122 CPS, indicated the dominance of the (104) plane in crystal orientation. The sharpness of the peaks, along with moderate broadening, confirmed the nanocrystalline nature of the synthesized particles. Using the Debye-Scherrer equation on the most intense peak, the estimated crystallite size of Fe_2O_3 nanoparticles fell within the 20–35 nm range, confirming successful synthesis in the nanorange. The absence of additional impurity peaks in the spectrum indicated the high purity of the synthesized Fe_2O_3 nanoparticles, making them promising for applications in catalysis, antimicrobial coatings and nano-enabled plant systems due to their stability and high surface area (Fig. 1).

The PXRD pattern of the prepared MgO nanoparticles showed sharp and well-defined peaks, clearly indicating that the particles were crystalline. Distinct peaks appeared around 37°, 43°, 63°, 75° and 79° (2θ), corresponding to the (111), (200), (220), (311) and (222) planes of cubic MgO, matching the standard reference (JCPDS card no: 45-0946) (8). The sharpness of these peaks reflected good crystallinity, while their slight broadening confirmed that the particles were in the nanoscale range (9). Using the Scherrer equation with the intense peak around 37° and Cu Kα radiation, the estimated crystallite size was around 18-25 nm, confirming the successful synthesis of MgO nanoparticles within the nanorange (10) (Fig. 2). Additionally, the absence of any extra peaks in the pattern indicated that the sample was pure and free from unwanted phases, confirming that the method used effectively produced clean MgO nanoparticles.

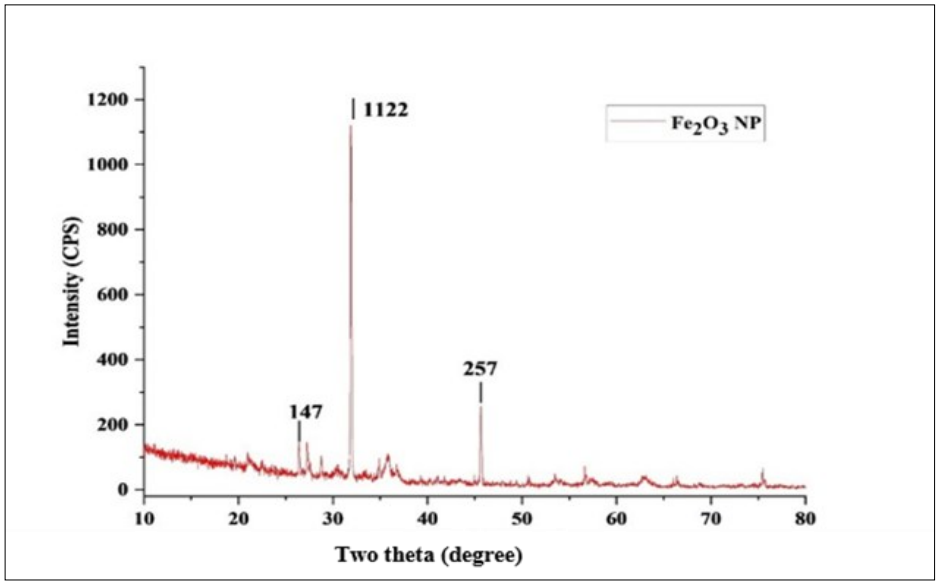

Fig. 1. XRD pattern of synthesized Fe_2O_3 nanoparticles showing sharp peaks corresponding to the rhombohedral structure, confirming crystallinity and phase purity.

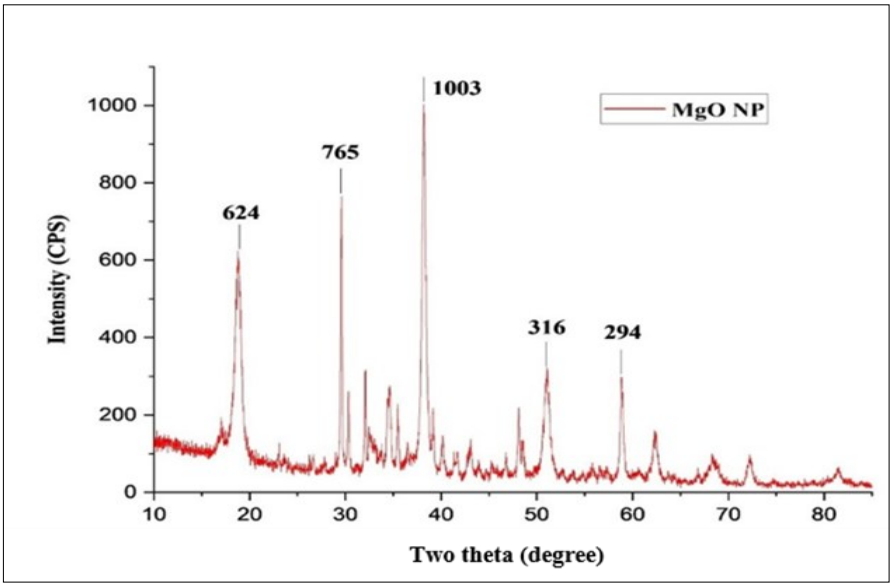

Fig. 2. XRD pattern of synthesized MgO nanoparticles showing sharp peaks corresponding to the cubic phase of MgO, confirming high crystallinity and purity with an estimated crystallite size of 18-25 nm.

Functional group characterization of Fe_2O_3 by FTIR

The FTIR spectrum of the synthesized Fe_2O_3 nanoparticles indicated the presence of key functional groups and confirmed the successful formation of iron oxide nanoparticles. A broad band at 3280 cm^{-1} corresponded to O-H stretching vibrations, indicating the presence of surface hydroxyl groups and adsorbed water on the nanoparticle surfaces. The peak at 1635 cm^{-1} was attributed to O-H bending vibrations, further confirming water molecules associated with the nanoparticles. A smaller peak at 1507 cm^{-1} may have corresponded to minor C=C or C-O stretching vibrations, potentially arising from plant extract residues or synthesis precursors. Importantly, strong absorption bands at 555 cm^{-1} and 405 cm^{-1} were characteristic of Fe-O stretching vibrations in Fe_2O_3, confirming the successful formation of iron oxide nanoparticles (11). The confirmation of hydroxyl groups suggested their role in plant interactions through electrostatic attraction, ligand exchange, reactive oxygen species modulation and signaling pathways. The presence of these peaks indicated that the Fe_2O_3 nanoparticles were well formed, possessed a reactive surface and maintained stability, making them suitable for incorporation into emulsion systems (Fig. 3, Table 1).

The FTIR spectrum of the synthesized MgO nanoparticles displayed several distinct peaks confirming the presence of surface functional groups and the formation of MgO. A broad absorption band around 3270 cm^{-1} was attributed to O-H stretching vibrations from adsorbed water molecules and surface hydroxyl groups on the nanoparticles, which were common due to atmospheric moisture during synthesis (12). The weak band at 2116 cm^{-1} may have corresponded to C-C stretching vibrations from trace organic residues or atmospheric CO_2. Peaks observed at 1636 cm^{-1} and 1508 cm^{-1} were due to O-H bending and possible C=O stretching vibrations, indicating the presence of surface-bound water and minor organic residues. The band at 1456 cm^{-1} was associated with C-H bending vibrations from residual capping agents or plant extracts used during green synthesis. Importantly, a strong absorption band around 411 cm^{-1} corresponded to the Mg-O stretching vibration, confirming the formation of MgO nanoparticles (13). The clear presence of these functional groups and the Mg-O stretching confirmed successful synthesis while indicating potential interaction sites, enhancing the dispersion of MgO nanoparticles (Fig. 4 and Table 2).

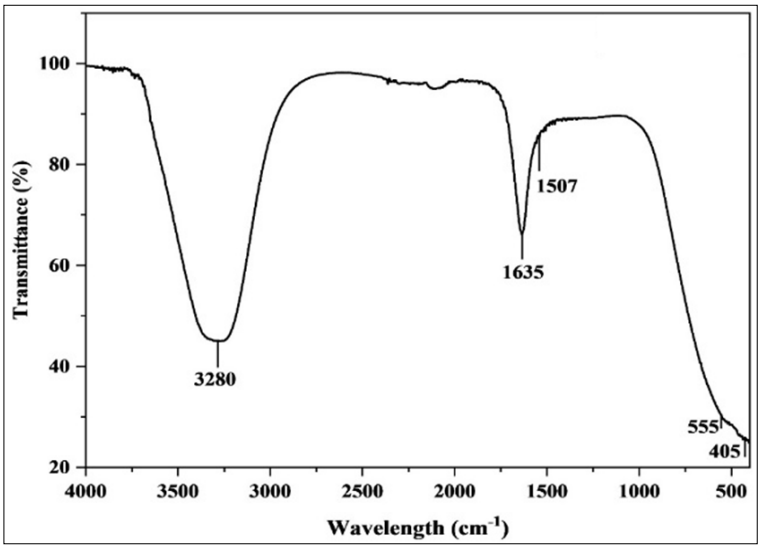

Fig. 3. FTIR spectrum of Fe_2O_3 nanoparticles showing O-H and Fe-O vibrational bands confirming nanoparticle formation.

Table 1. FTIR analysis of Fe_2O_3 nanoparticles showing peak positions and corresponding functional groups

Peak (cm^{-1})	Detected vibration	Functional group
3280	O–H stretching	Surface hydroxyl groups / adsorbed water
1635	O–H bending	Adsorbed water molecules
1507	C=C or C–O stretching	Possible plant extract residues (minor)
555	Fe–O stretching	Fe_2O_3 nanoparticle confirmation
405	Fe–O stretching	Fe_2O_3 nanoparticle confirmation

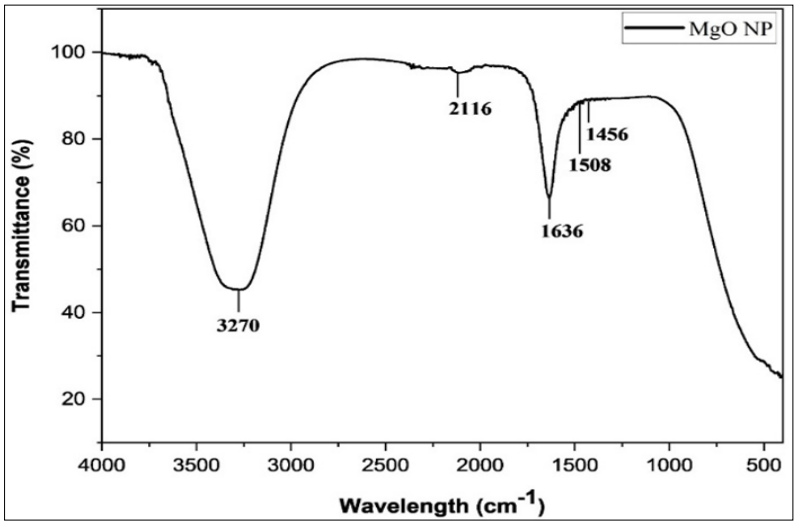

Fig. 4. FTIR spectrum of synthesized MgO nanoparticles showing characteristic O-H, C-H, C=O and Mg-O vibrational bands, confirming surface functionalities and formation of MgO.

Table 2. FTIR analysis of MgO nanoparticles showing peak positions and corresponding functional groups

Peak (cm^{-1})	detected vibrations	functional group
3270	O–H stretching	Surface hydroxyl, adsorbed water
2116	C≡C stretching / CO_2	Residual organic moieties / atmospheric CO_2
1636	O–H bending	Adsorbed water
1508	C=O stretching	Minor organic residues
1456	C–H bending	Residual organic/capping agents
411	Mg–O stretching	MgO confirmation

Structural and morphological analysis of Fe_2O_3 by TEM

The TEM image of the synthesized Fe_2O_3 nanoparticles showed a moderately agglomerated structure with particles clearly visible within the nanoscale range. The measured particle sizes vary from 22.8 nm to 64.3 nm, confirming the successful formation of Fe_2O_3 nanoparticles with heterogeneous yet controlled size distribution. The particles exhibit an irregular near-spherical to polyhedral morphology, which is commonly observed for Fe_2O_3 synthesized via wet chemical routes, indicating good crystallinity supported by XRD analysis. The observed clustering can be attributed to the high surface energy and magnetic properties of Fe_2O_3 nanoparticles, leading to slight aggregation during the drying process. This agglomeration may overcome through process called surface functionalization using inorganic coatings (Silica, Carbon, Polymers) and organic coatings (citric acid, oleic acid, amines, thiols and phosphates). The clear edges and distinct boundaries in the TEM image confirm the crystalline nature and nano-range of the synthesized Fe_2O_3, making them potentially suitable for emulsion system where high surface area and reactivity are advantageous (Fig. 5).

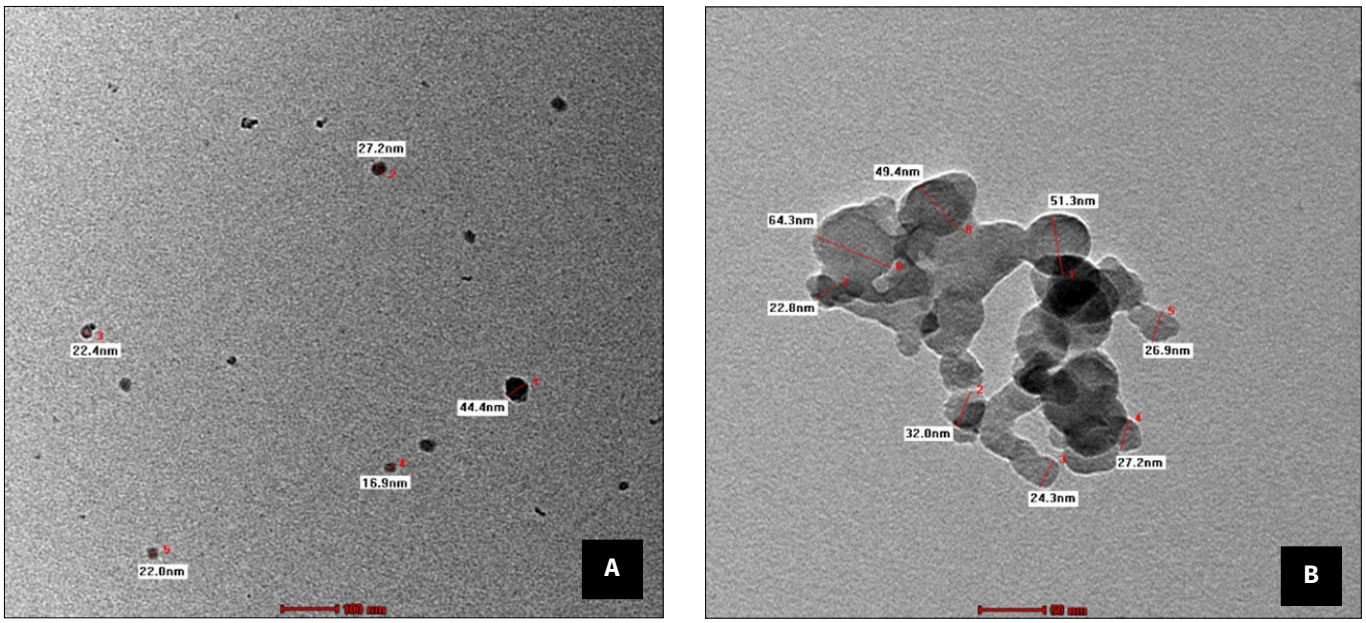

Fig. 5. A and B show TEM image of Fe_2O_3 nanoparticles showing particle sizes in the range of 22.8-64.3 nm with polyhedral morphology and moderate aggregation.

The TEM image of the synthesized MgO nanoparticles shows well dispersed particles with a predominantly hexagonal morphology, confirming the controlled synthesis achieved in the preparation process. The particles appear with clear, sharp edges and uniform contrast, indicating high crystallinity and phase purity consistent with the XRD results. The particle sizes are observed within the range of 20-40 nm, aligning closely with the nanorange estimated from XRD analysis, while the slight agglomeration seen in a few areas is typical for oxide nanoparticles due to their high surface energy (14) (Fig. 6). The hexagonal shape of these MgO nanoparticles can contribute to a higher surface area and improved reactivity, which is beneficial for enhancing dispersion stability in all systems and increasing interaction with any surfaces. Additionally, the clear visibility of particle boundaries without significant deformation suggests effective synthesis and minimal structural defects, making these hexagonally shaped MgO nanoparticles (15).

Conclusion

This study demonstrates the successful green synthesis of Fe_2O_3 and MgO nanoparticles exhibiting confirmed crystallinity, surface reactivity and nanoscale morphology. The synthesized nanoparticles exhibited promising physicochemical properties that make them well-suited for diverse applications, including catalysis, antimicrobial coatings and nano-enabled agricultural systems. Their magnetic and surface characteristics suggest potential for advanced uses such as targeted delivery and environmental remediation, aligning with sustainable nanotechnology goals. The eco-friendly biosynthesis enhances biocompatibility and reduces environmental impact, supporting the development of functional nanomaterials for practical applications in science and industry. The successfully synthesized nanoparticles show ideal properties for further investigation into their efficacy as nano-fertilizers or antimicrobial agents against plant pathogens.

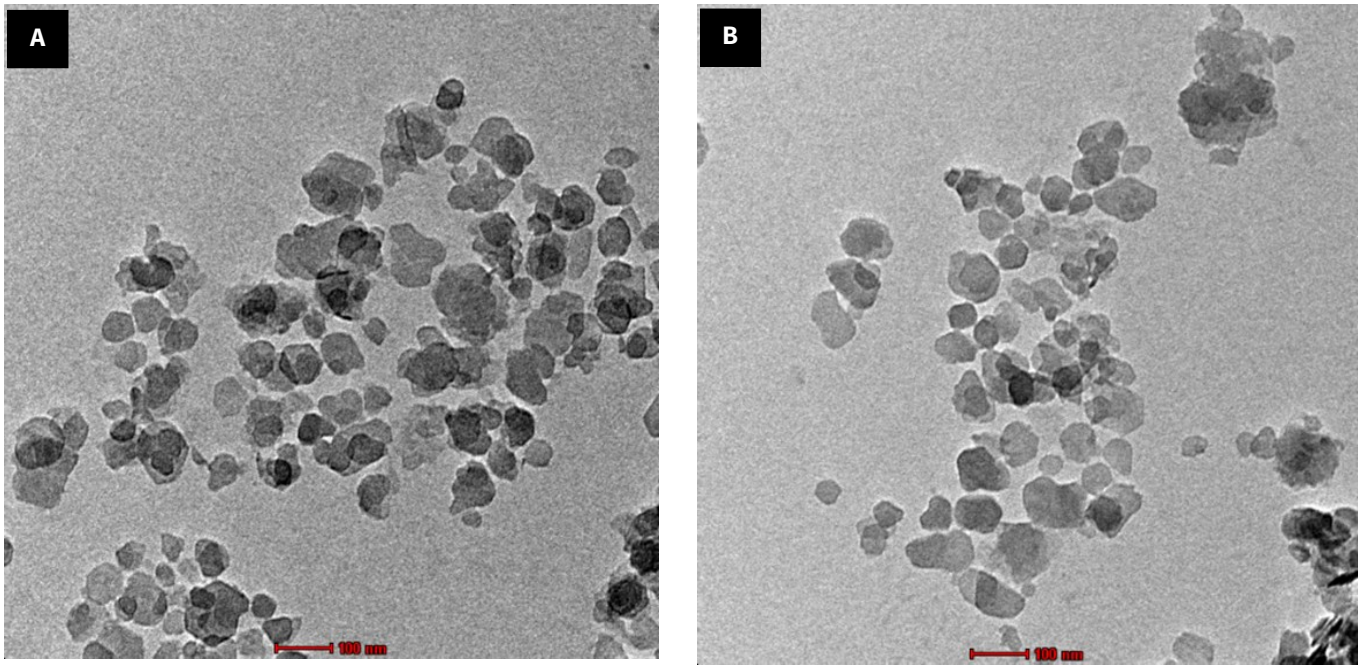

Fig. 6. A and B show TEM image of synthesized MgO nanoparticles exhibiting predominantly hexagonal morphology with particle sizes in the range of 20-40 nm, confirming high crystallinity and uniform dispersion.

Acknowledgements

The authors gratefully acknowledge the Centre for Agricultural Nanotechnology, Tamil Nadu Agricultural University, Coimbatore, India.

Authors' contributions

RR and KA led writing the original draft, review and editing. PSM provided supervision and conceptualization. MR, GK, VG and MD involved in supervision. All authors read and approved the final manuscript.

Compliance with ethical standards

Conflict of interest: Authors do not have any conflict of interests to declare.

Ethical issues: None

Declaration of generative AI and AI-assisted technologies in the writing process:

During the preparation of this work, the authors utilised ChatGPT by OpenAI to assist with language refinement for clarity. After using this tool, the authors reviewed, validated and edited the content as needed and take full responsibility for the integrity and accuracy of the final version of the publication.

References

1. Abiodun AJ, Alamu GA, Adedokun O, Abati SM, Sanusi YK. Enhancing photovoltaic performance of monolithic dye-sensitized solar cells through green-synthesized CuO-FeO nanocomposite counter electrodes. Sustainable Energy Res. 2024;11(1):46. https://doi.org/10.1186/s40807-024-00139-7
2. Jegadeesan GB, Srimathi K, Srinivas NS, Manishkanna S, Vignesh D. Green synthesis of iron oxide nanoparticles using *Terminalia bellirica* and *Moringa oleifera* fruit and leaf extracts: antioxidant, antibacterial and thermoacoustic properties. Biocatal Agric Biotechnol. 2019;21:101354. https://doi.org/10.1016/j.bcab.2019.101354
3. Poh Yan L. Greener synthesis of nanostructured iron oxide for medical and sustainable agro-environmental benefits. Front Chem. 2022;10:984218. https://doi.org/10.3389/fchem.2022.984218
4. Jadhav V, Bhagare A, Ali IH, Dhayagude A, Lokhande D, Aher J, et al. Role of *Moringa oleifera* on green synthesis of metal/metal oxide nanomaterials. J Nanomater. 2022;2022:2147393. https://doi.org/10.1155/2022/2147393
5. Ahmad S, Ahmad N, Islam MS. Rice seeds biofortification using biogenic iron oxide nanoparticles synthesized by using *Glycyrrhiza glabra*: a study on growth and yield improvement. Sci Rep. 2024;14(1):12368. https://doi.org/10.1038/s41598-024-62907-1
6. Kiwumulo HF, Muwonge H, Ibingira C, Lubwama M, Kirabira JB, Sekitoleko RT. Iron oxide nanoparticles in leukemia: design, diagnostic applications and therapeutic strategies. JENCI. 2025;37(1):44.
7. Fellner P. Preparation of magnesium hydroxide from nitrate aqueous solution. Chem Pap. 2011;65(4):454-9.
8. Hussain A, Yasar M, Ahmad G, Ijaz M, Aziz A, Nawaz MG, et al. Synthesis, characterization and applications of iron oxide nanoparticles. IJHS. 2023;17(4):3.
9. Sutapa IW, Wahab AW, Taba P, La Nafie N. Synthesis and structural profile analysis of the MgO nanoparticles produced through the sol-gel method followed by annealing process. OJC. 2018;34(2):1016.
10. Rotti RB, Sunitha K, Manjunath M, Roy N, Mayegowda N, Gnanaprakash K, et al. Green synthesis of MgO nanoparticles and its antibacterial properties. Front Chem. 2023;11:1143614. https://doi.org/10.3389/fchem.2023.1143614
11. Khodair T, Abed H, Majeed G. Synthesis and structural characterization of MgO nanoparticles. IJARSET. 2016;3(7):2400-6.
12. Munjal S, Singh A, Kumar V. Synthesis and characterization of MgO nanoparticles by orange fruit waste through green method. IJARCS. 2017;4(9):36-42.
13. Radulescu DM. Green-synthesized MgO nanoparticles: structural insights and antimicrobial applications. IJMS. 2025;26(18):9021.
14. Daniele V, Volpe AR, Cesare P, Taglieri G. MgO nanoparticles obtained from an innovative and sustainable route and their applications in cancer therapy. Nanomaterials. 2023;13(22):2975.
15. Abbas IK, Adim KA. Synthesis and characterization of magnesium oxide nanoparticles by atmospheric non-thermal plasma jet. KJS. 2023;50(3):223-30.

Additional information

Peer review: Publisher thanks Sectional Editor and the other anonymous reviewers for their contribution to the peer review of this work.

Reprints & permissions information is available at https://horizonepublishing.com/journals/index.php/PST/open_access_policy

Publisher's Note: Horizon e-Publishing Group remains neutral with regard to jurisdictional claims in published maps and institutional affiliations.

Indexing: Plant Science Today, published by Horizon e-Publishing Group, is covered by Scopus, Web of Science, BIOSIS Previews, Clarivate Analytics, NAAS, UGC Care, etc
See https://horizonepublishing.com/journals/index.php/PST/indexing_abstracting

Publisher information: Plant Science Today is published by HORIZON e-Publishing Group with support from Empirion Publishers Private Limited, Thiruvananthapuram, India.